

Characterization of a sodium-cooled fast reactor in an MHR–SFR synergy for TRU transmutation

Ser Gi Hong^a, Yonghee Kim^{a,*}, Francesco Venneri^b

^a Korea Atomic Energy Research Institute, 150 Deokjin-dong, Yuseong, Daejeon 305-353, Republic of Korea

^b General Atomics, P.O. Box 85608, San Diego, CA, USA

Received 21 July 2007; received in revised form 13 January 2008; accepted 16 January 2008

Available online 5 March 2008

Abstract

In the task of destroying the light water reactor (LWR) transuranics (TRUs), we consider the concept of a synergistic combination of a deep-burn (DB) gas-cooled reactor followed by a sodium-cooled fast reactor (SFR), as an alternative way to the direct feeding of the LWR TRUs to the SFR. In the synergy concept, TRUs from LWR are first deeply incinerated in a graphite-moderated DB-MHR (modular helium reactor) and then the spent fuels of DB-MHR are recycled into the closed-cycle SFR. The DB-MHR core is 100% TRU-loaded and a deep-burning (50–65%) is achieved in a safe manner (as discussed in our previous work). In this analysis, the SFR fuel cycle is closed with a pyro-processing technology to minimize the waste stream to a final repository. Neutronic characteristics of the SFR core in the MHR–SFR synergy have been evaluated from the core physics point of view. Also, we have compared core characteristics of the synergy SFR with those of a stand-alone SFR transuranic burner. For a consistent comparison, the two SFRs are designed to have the same TRU consumption rate of ~ 250 kg/GW EFPY that corresponds to the TRU discharge rate from three 600 MW DB-MHRs. The results of our work show that the synergy SFR, fed with TRUs from DB-MHR, has a much smaller burnup reactivity swing, a slightly greater delayed neutron fraction (both positive features) but also a higher sodium void worth and a less negative Doppler coefficients than the conventional SFR, fed with TRUs directly from the LWRs. In addition, several design measures have been considered to reduce the sodium void worth in the synergy SFR core.

© 2008 Elsevier Ltd. All rights reserved.

1. Introduction

Sodium-cooled fast reactors (SFR) have potential in the transmutation of the transuranic nuclides (TRUs) and some fission products discharged from LWRs (Wakabayashi et al., 1997; Hill et al., 1995). The hard neutron spectrum of the fast reactor makes it possible for the neutrons to undergo effectively a fission reaction rather than a capture one which results in formation of higher actinides. Also, more surplus neutrons per fission are available in the fast spectrum reactors than in the thermal ones even if the parasitic capture and the leakage are considered (Messaoudi and Tommasi, 2002). And the surplus neutrons can be used

for additional transmutation of radioactive fission products such as Tc-99 in the reflector region. However, when an SFR is loaded with only reactor-grade TRU fuels to maximize the transmutation performance, there are several design challenges such as a large reactivity swing and a smaller delayed neutron fraction, which require a more elaborate reactor control system. To mitigate such problems, natural (or depleted) uranium is often added to the fuel, but these results in a relatively low fuel burnup. A low discharge burnup implies a large amount of spent fuel to be repeatedly reprocessed to close the fuel cycle.

Recently, the deep-burn (DB) concept using a graphite-moderated modular helium reactor (MHR) has been studied as a way to accomplish the destruction and utilization of spent fuel transuranics (TRU) (Baxter et al., 2001; Kim and Venneri, 2007). In this concept, ceramic-coated particle fuels (TRISO) are used and deep-burning (typically 50–

* Corresponding author. Tel.: +82 42 868 2067; fax: +82 42 868 8917.
E-mail address: yhkim@kaeri.re.kr (Y. Kim).

65%) of TRUs are feasible in a single irradiation campaign without repeated reprocessing (Kim and Venneri, 2007). The moderation by graphite produces valuable opportunities for thermal and epithermal neutrons to interact with fissionable and non-fissionable materials. In particular, the moderation by graphite allows for an effective use of the resonance absorption of ^{240}Pu to counteract the reactivity feedback of ^{239}Pu . The achievement of the TRU deep-burn in MHR is mainly due to the following reasons: (1) the use of uranium-free fuel and low inventory of heavy metal, (2) the effective conversion of ^{240}Pu to ^{241}Pu , and (3) the robust fuel characteristics of the TRISO fuel. Because deep-burn is a single pass operation, after irradiation, still a significant amount of spent fuel (deep-burn TRISO) would need to be disposed of in a final repository in a deep-burn stand-alone scenario, as the fuel cycle is extended, but not closed.

In this paper, a synergistic combination of the DB-MHR and an SFR burner is considered for a safe and efficient transmutation of the TRUs from LWRs. In this MHR–SFR synergy, the fuel cycle is closed with an SFR burner: the spent fuel of DB-MHR is reprocessed and recycled into the SFR, providing a fuel cycle extension and true closure. Fig. 1 shows the concept of the LWR–MHR–SFR combined fuel cycle for the TRU transmutation. The recovered LWR TRUs are deep-burned in 600 MWt MHRs and the remaining TRUs are additionally incinerated in an SFR after a reprocessing with a pyro-technology, in which only fission products are removed. For reprocessing of the MHR spent fuel, the coating layers of TRISO particles are cracked and removed through a milling process that produces exposed oxide kernels (Del Cul et al., 2002). The recovered kernels can be reprocessed by using a pyroprocess for an oxide fuel (Vavilov et al., 2004). It should be mentioned that the reprocessing technologies are not fully developed, but under development.

The thermal power and the core design parameters of the SFR transmuter are determined to have a TRU consumption rate of $\sim 250 \text{ kg/GWtEPY}$ that roughly corresponds to the TRU discharge rate from three 600 MWt DB-MHRs providing $\sim 60\%$ TRU burnup. An MHR–SFR synergy system based on these operation parameters can support roughly 10 GWt of LWRs.

The MHR–SFR synergy may provide several advantages over either the stand-alone DB-MHR or SFR approach. The front-end deep-burning in an MHR reduces substantially the number of SFR burners required, and thus a relatively fast TRU transmutation is feasible with significantly reduced reprocessing needs. In addition, the fission energy from the TRUs can be used more efficiently due to the very high thermal efficiency of an MHR ($\sim 48\%$ for MHR and $\sim 38\%$ for SFR) and the extremely high burnup of the DB-MHR fuel ($>600,000 \text{ MWD/t}$).

The objective of this paper is to evaluate the core performance parameters of the SFR burner in the MHR–SFR synergy concept and to compare them with a conventional SFR core directly loaded with LWR TRUs.

In Section 2, the computational models and core design descriptions are provided. Section 3 gives the core performance analysis results. In Section 4, we explore design measures to reduce the sodium void worth. Finally, the summary and conclusion are given in Section 5.

2. Computational models and core design description

2.1. Computational models and assumptions

The core depletion analysis is done using the equilibrium model of the REBUS-3 code system (Toppel, 1983) in which the DIF3D (Derstine, 1984) module solves the neutron diffusion equation with a HEX-Z nodal method and a

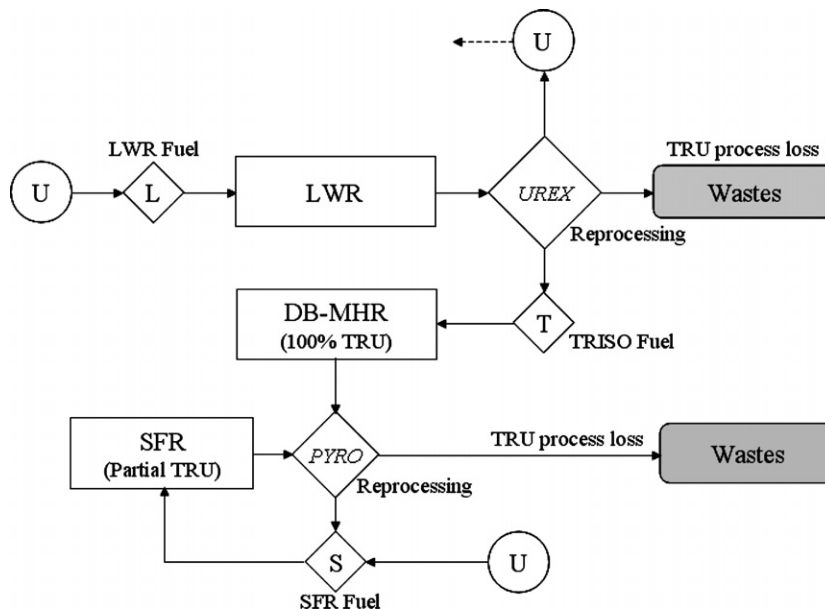


Fig. 1. Fuel cycle concept of the MHR–SFR synergy scenario.

nine-group cross section set to obtain the neutron flux and power distributions. The cross section set is based on the

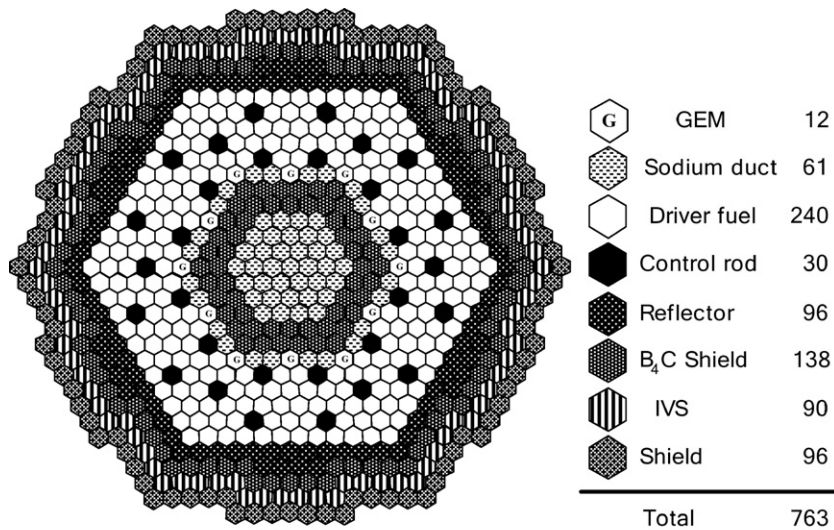
Table 1
Comparison of the feed TRU compositions (wt%)

Nuclides	TRU from LWR	TRU from DB-MHR
²³⁴ U	–	1.00
²³⁵ U	–	0.05
²³⁶ U	–	0.02
²³⁷ Np	6.8	7.11
²³⁸ Pu	2.9	16.74
²³⁹ Pu	49.5	2.66
²⁴⁰ Pu	23.0	10.79
²⁴¹ Pu	8.8	9.86
²⁴² Pu	4.9	30.89
²⁴¹ Am	2.8	4.01
^{242m} Am	0.02	0.07
²⁴³ Am	1.4	10.26
²⁴² Cm	–	0.00
²⁴³ Cm	–	0.04
²⁴⁴ Cm	–	5.95
²⁴⁵ Cm	–	0.45
²⁴⁶ Cm	–	0.10

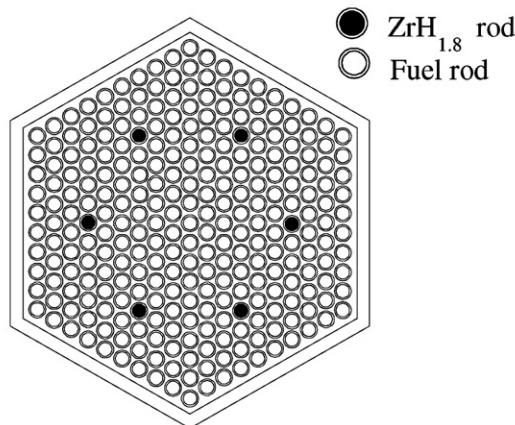
ENDF/B-VI library. The starting library is a microscopic 150 group cross section file (Kim, 2001) in the MATXS format. The TRANSX (MacFARLANE, 1993) code is used to obtain the ISOTXS format of the multi-group cross sections. All the reactivity coefficients and worth are calculated by using the DIF3D HEX-Z nodal method with 80-group cross section data.

A 4-batch fuel management scheme is used and a 14-month cooling time is assumed for reprocessing. It is assumed that 0.1% of TRU is lost during reprocessing and 5% of the rare-earth (RE) fission products are carried over to the next cycle. The reprocessed fuel materials are sent to the fuel fabrication facility where they are blended with the external feed materials (a mixture of the TRU nuclides discharged from the LWR or DB-MHR and depleted uranium).

Table 1 compares LWR and DB-MHR TRU vectors used in this work. For the LWR TRU feed, a 50 GWD/tU burnup and a 5-year cooling were assumed. All Cm isotopes (mostly Cm-244, $T_{1/2} = 18.11$ years) are assumed to



(a) Core configuration



(b) Assembly configuration

Fig. 2. Configuration of the SFR core and fuel assembly.

be removed, which are to be stored for natural decay to plutonium (mostly Pu-240). The resulting plutonium can be effectively used as a fertile fuel in the DB-MHR or it can be fed into the SFR, which was not considered in this work since its impact on the core performance is only marginal due to a very small Cm fraction ($\sim 0.2\%$) in the PWR TRU feed. The DB-MHR TRU vector was obtained by assuming a 63.5% burnup and a 5-year cooling (Kim and Venneri, 2007). It should be noted that only fission products are removed from the DB-MHR spent fuel and a small amount of uranium is contained in the TRU feed vector from the DB-MHR. In Table 1, it is noted that the DB-MHR TRU vector has higher fractions of ^{238}Pu , ^{241}Pu , ^{242}Pu , ^{243}Am , ^{244}Cm and a significantly lower content of ^{239}Pu than the LWR TRU.

2.2. Core design description

The SFR transmutation reactor core rates 1500 MWt. The core configuration (Hong et al., 2008) is shown in Fig. 2, and Table 2 summarizes the main core design parameters. As shown in Fig. 2, the core is a homogeneous annular type and there is a large central non-fuel region. The central region is introduced to reduce the conversion ratio so as to achieve high transmutation capability, to reduce the sodium void worth and to achieve power flattening without an enrichment splitting. A relatively short core height (80 cm) is adopted in the core design to improve the sodium void worth. There are 240 fuel assemblies in the core.

The first four rings (1st, 2nd, 3rd, and 4th rings) consist of sodium ducts comprised of duct and sodium coolant. Two rings (5th and 6th rings) are occupied with B_4C shield assemblies in order to effectively absorb the neutrons leaking from the core. The last ring of the central island consists of sodium ducts and gas expansion modules (GEMs). The sodium duct positions in this ring can be replaced by control assemblies, if necessary. Each fuel

Table 2
The main core design parameters

Parameters	Values
Power (MWt)	1500
Cycle length (EFPD)	332
Number of fuel management batches	4
Active fuel length (cm)	80
Number of rods/FA	271
Number of fuel rods/FA	265
Number of $\text{ZrH}_{1.8}$ rods/FA	6
Structural material	HT9
Assembly pitch (cm)	16.57
Fuel type	TRU-U-Zr
Fuel smear density	75%TD
Rod outer diameter (mm)	7.5
Clad thickness (mm)	0.53
Wire wrap diameter (mm)	1.60
P/D ratio	1.23
Volume fractions (%) of fuel assembly	36.3/38.9/24.0
Fuel/coolant/structure	

assembly has six moderator ($\text{ZrH}_{1.8}$) rods to soften the neutron spectrum. The moderator rods are used to improve the Doppler coefficient, to reduce peak fast neutron fluence, and to reduce the sodium void worth. The $\text{ZrH}_{1.8}$ is used in this study since it provides a relatively good neutron moderation. However, the operating temperature of the zirconium hydride is limited by about 550 C due to the irradiation-induced disintegration, while the temperature limit is much higher (~ 1000 C) for an yttrium hydride (Newton and Smith, 2003). Our experience reveals that an yttrium hydride provides a similar neutronic performance. We have found that the moderator rods make the local power peaking only slightly higher as shown in Section IV. The fuel is a metallic alloy of TRU-U-Zr including a small amount of RE elements.

3. Core performance analysis

In this section, we have analyzed and compared the two SFR cores fed with LWR and DB-MHR TRUs, respectively. The core configuration and all the design parameters except for the fuel composition in fuel are identical for the two cores. The Zr content is adjusted so that the two cores have the same TRU consumption rate, i.e., ~ 250 kg/GWtEFPY. For the case of the core fed with LWR TRU, this TRU consumption rate corresponds to the TRU discharge rate from ~ 2.5 LWRs of the same power rating (i.e., 1500 MW t). The core cycle length is 332 EFPDs.

Table 3 summarizes the performance of the cores. As shown in Table 3, the core with an MHR TRU feed has a higher TRU content and a lower Zr content than in a LWR TRU feed. This is because the MHR TRU contains

Table 3
Comparison of the core performances

Parameters	CORE-I (PWR TRU)	CORE-II (DB-MHR TRU)
Charge composition (wt%) TRU/U/RE fission products/Zr	37.6/43.3/0.12/19.0	45.48/42.6/ 0.11/11.8
Burnup reactivity swing (pcm)	5091	2851
Conversion ratio (fissile)	0.5625	0.8651
Conversion ratio (TRU)	0.5634	0.6175
Average discharge burnup (MWD/kg)	143.1	119.0
Charged/discharged TRU masses (kg)	1573.6/1233.0	2100.6/1761.7
Charged/discharged U masses (kg)	1814.9/1639.7	1968.2/1789.2
TRU wt% in HM (BOEC/EOEC)	45.1/44.2	50.88/50.38
TRU inventory (kg, BOEC/EOEC)	5742/5401	7872/7533
U inventory (kg, BOEC/EOEC)	6991.1/6815.9	7599/7420
TRU consumption (kg/GWtEFPY)	251.5	251.9
U consumption (kg/GWtEFPY)	127.5	129.1
Average power density (W/cc)	301.7	302.1
Average linear heat rate (W/cm)	279.0	279.1
3D power peaking factor (BOEC/ EOEC)	1.41/1.37	1.47/1.44
Peak fast neutron fluence (n/cm^2)	3.45×10^{23}	3.45×10^{23}

a much lower fissile content than the LWR TRU feed. The lower Zr content of the MHR TRU core means a higher fuel loading and a lower discharge burnup is achieved in the MHR TRU core by ~17% than in the LWR TRU core.

In the conventional metallic alloy of U–Pu–Zr, the Zr content is usually fixed at 10% and the Pu content is often less than 30% (Hill et al., 1995; Hofman et al., 1997). In the two SFR cores, Table 3 indicates that TRU content is much higher than 30% for both cases and Zr content is also significantly different from the typical value of 10%. These features may raise feasibility issues of the fuels in Table 3, which is beyond the scope of this work.

It is interesting to see that the MHR TRU core provides a much higher fissile conversion ratio than the LWR TRU core, while the two cores have quite comparable TRU conversion ratio. As a result of the higher fissile conversion ratio, the MHR TRU core has a significantly lower value of burnup reactivity swing, by ~2200pcm (i.e., ~7%) than that of the LWR TRU core. This is an important advantage in designing a high-performance TRU burner because the lower burnup reactivity swing reduces the burden of the control assemblies and improves the core safety. It is well known that a large burnup reactivity swing is one of the challenging problems in designing the SFR TRU transmuter with its small delayed neutron fraction, and a relatively short cycle length is usually adopted due to the large reactivity swing.

Table 3 also shows that both cores consume quite comparable amount of uranium. The two cores have reasonably low values of the 3-D power peaking factor and the discharge fast neutron fluence is sufficiently lower than the radiation damage limit (~4.0 × 10²³ n/cm²) of the HT-9 cladding (Leggett and Walters, 1993).

Fig. 3 compares the normalized assembly-wise power distributions of the two cores at beginning of equilibrium cycle (BOEC). It is observed that there is no significant difference in the power distribution. However, the power density in the core boundary region is lower in the MHR TRU case.

Table 4 compares the compositions of TRU at BOEC. Table 4 shows that the core fed with TRU from DB-MHR has a higher content of total minor actinide (in particular, ²⁴³Am and ²⁴⁴Cm) and ²⁴²Pu. Table 5 compares the neutron balance in the active core region both for the

Table 4
Comparison of the compositions (wt%) of TRU nuclides at BOEC

Nuclides	CORE-I (PWR TRU)	CORE-II (DB-MHR TRU)
²³⁸ Pu	4.85	8.00
²³⁹ Pu	31.67	12.87
²⁴⁰ Pu	35.14	19.44
²⁴¹ Pu	6.02	3.87
²⁴² Pu	9.29	27.58
²³⁷ Np	3.03	2.60
²⁴¹ Am	3.93	3.25
^{242m} Am	0.27	0.23
²⁴³ Am	2.90	10.31
²⁴² Cm	0.15	0.11
²⁴³ Cm	0.02	0.02
²⁴⁴ Cm	1.90	8.08
²⁴⁵ Cm	0.56	2.42
²⁴⁶ Cm	0.26	1.20
Plutonium	86.97	71.77
Minor actinide	13.03	28.23

Table 5
Comparison of the neutron balances at BOEC

Type	CORE-I (PWR TRU)		CORE-II (DB-MHR TRU)	
	Sodium flooded	Sodium voiding	Sodium flooded	Sodium voiding
Leakage	0.953	1.040	0.922	0.991
Planar	0.562	0.595	0.547	0.569
Axial	0.391	0.445	0.376	0.422
Fission	1.000	1.000	1.000	1.000
Capture	0.886	0.793	1.071	0.952
²³⁸ U	0.2643	0.2424	0.2640	0.2397
²³⁸ Pu	0.0282	0.0255	0.0587	0.0527
²³⁹ Pu	0.1228	0.1067	0.0614	0.0530
²⁴⁰ Pu	0.1334	0.1188	0.0934	0.0826
²⁴¹ Pu	0.0210	0.0188	0.0170	0.0151
²⁴² Pu	0.0307	0.0275	0.1144	0.1016
²³⁷ Np	0.0374	0.0333	0.0405	0.0357
²⁴¹ Am	0.0512	0.0455	0.0533	0.0470
^{242m} Am	0.0006	0.0005	0.0006	0.0005
²⁴³ Am	0.0338	0.0300	0.1504	0.1327
²⁴² Cm	0.0004	0.0004	0.0004	0.0003
²⁴³ Cm	0.0000	0.0000	0.0000	0.0000
²⁴⁴ Cm	0.0124	0.0112	0.0666	0.0594
²⁴⁵ Cm	0.0013	0.0012	0.0073	0.0065
²⁴⁶ Cm	0.0005	0.0004	0.0028	0.0025
(n,2n)	0.003	0.003	0.004	0.004
ν	2.993	2.998	3.091	3.095

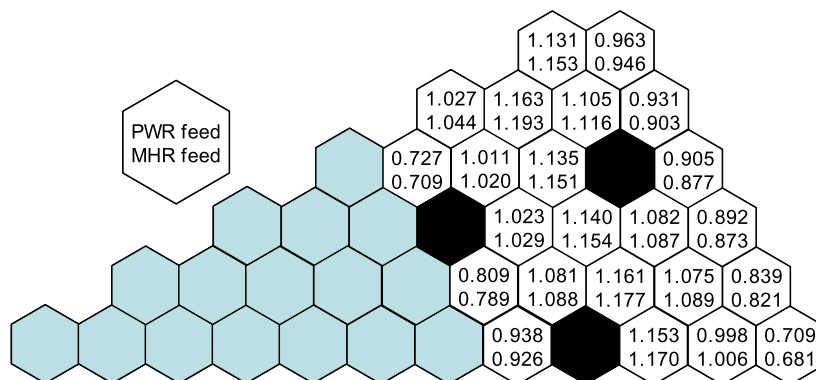


Fig. 3. Comparison of the assembly-wise power distribution at BOEC.

sodium-flooded and sodium-voiding cases. In this table, all the reaction and leakage rates are normalized to a unit fission rate. Table 5 shows that the DB-MHR TRU core has a smaller leakage rate and a noticeably higher capture rate than the core fed with LWR TRU.

In general, the core safety features strongly depend on the neutron spectrum. Fig. 4 compares the neutron spectra of the two cores. The neutron spectrum is a little harder in the DB-MHR TRU core. This can be ascribed to the fact that the DB-MHR TRU core has higher capture probabilities for relatively low energy neutrons because it has a higher content of minor actinides.

Table 6 compares the reactivity coefficients and the reactivity worth of control assemblies. From this table, the followings are observed: The core fed with DB-MHR TRU has (1) a less negative Doppler coefficient, (2) a less negative radial expansion reactivity coefficient of the core sup-

port structure, (3) a more negative axial expansion of the fuel, (4) a more positive sodium void worth by $\sim 4.4\%$ for sodium voiding in the core plus gas plenum, (5) a smaller control assembly worth by ~ 2200 pcm at BOEC, (6) a slightly larger effective delayed neutron fraction, and (7) a shorter neutron life time than the core fed with LWR TRU.

The less negative Doppler coefficient of the DB-MHR TRU core is a combined effect of a harder neutron spectrum and a larger minor actinide inventory. The two cores have sodium void worth of 1.3\$ and 5.7\$ at BOEC for the sodium voiding in the active core plus gas plenum, for the LWR TRU and the DB-MHR TRU, respectively. The more positive sodium void worth of the MHR TRU core is due to the harder neutron spectrum and a higher minor actinide content. The inclusion of the sodium voiding in 12 GEMs give a negative sodium void worth of -0.4% for the LWR TRU core, while the sodium void worth is still positive for the DB-MHR TRU core.

Also, it is noted in Table 5 that the sodium voiding leads to a smaller increase of leakage probability and a larger decrease of capture probability in the DB-MHR TRU core than in the LWR TRU core. This explains why the MHR TRU core has a larger sodium void worth. Among TRU nuclides, ^{237}Np , ^{240}Pu , ^{242}Pu , ^{241}Am , ^{243}Am , ^{242}Cm , ^{244}Cm , and ^{246}Cm have higher increase rates in the η values resulting from spectrum hardening by sodium voiding. A core with higher contents of these nuclides usually has a higher sodium void worth. The main reason of the increased η value is the increased fission-to-capture ratio for most heavy nuclides. Table 5 also shows that the capture rates of most nuclides become smaller in the DB-MHR TRU core in the case of sodium voiding.

The harder neutron spectrum of the DB-MHR TRU core results in a lower control rod worth: 20.4\$ at BOEC, compared to 26.3\$ for LWR TRU core. However, taking into account the burnup reactivity swing, the DB-MHR

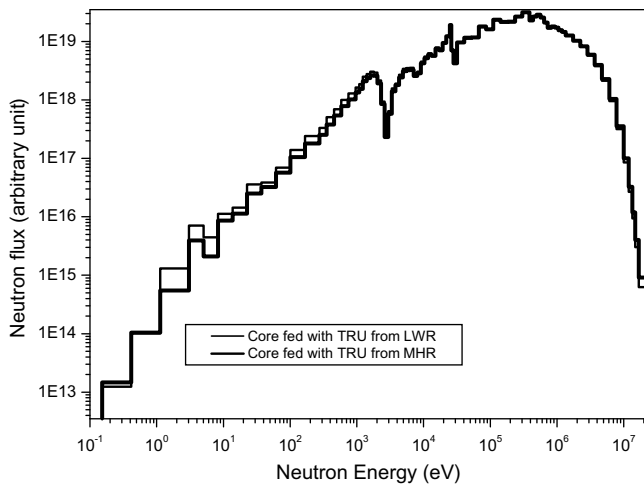


Fig. 4. Comparison of the core neutron spectrum.

Table 6
Comparison of the reactivity coefficients and reactivity worth

Parameters	CORE-I (PWR TRU)	CORE-II (DB-MHR TRU)
Fuel Doppler coefficient ($\Delta\rho/K$) (Na flooded)		
BOEC (at 900 K)	$-0.00279T^{-1.00}(-3.13 \times 10^{-6})$	$-0.00188T^{-1.02}(-1.82 \times 10^{-6})$
EOEC (at 900 K)	$-0.00290T^{-1.00}(-3.33 \times 10^{-6})$	$-0.00186T^{-1.01}(-1.93 \times 10^{-6})$
Radial expansion coefficient (pcm/%; pcm/K)	$-563^a/-600^b; -0.82^a/-0.88^b$	$-552^a/-572^b; -0.81^a/-0.83^b$
Fuel axial expansion coefficient		
Fuel only (pcm/%; pcm/K)	$-254^a/-274^b; -0.40^a/-0.43^b$	$-280^a/-292^b; -0.44^a/-0.46^b$
Fuel + clad (pcm/%)	$-226^a/-242^b$	$-231^a/-240^b$
Sodium density coefficient (pcm/K)	$0.01^a/0.13^b$	$0.53^a/0.55^b$
Sodium void worth (pcm)		
Core + gas plenum	$396^a/512^b$	$1777^a/1858^b$
Core + gas plenum + GEMs	$-133^a/-91^b$	$1331^a/1392^b$
Control assembly worth (pcm)	$7983^a/8610^b$	$6330^a/6658^b$
Effective delayed neutron fraction	$0.00304^a/0.00306^b$	$0.00310^a/0.00310^a$
Neutron life time (micro sec)	$0.356^a/0.371^b$	$0.288^a/0.299^b$

^a BOEC.

^b EOEC.

TRU core has a higher remaining rod worth of 11.2\$ compared with 9.6\$ of the LWR TRU core at BOEC. In the actual control rod design, several other factors should be considered additionally, which include two independent shutdown systems, temperature defect from the cold zero to hot-full power, stuck rod worth etc. In the present design, natural B₄C was used as the neutron absorber of control rods. For an increased control rod worth, enriched boron or more control assemblies can be used.

In an SFR for TRU burning, one of the safety concerns is the small value of the delayed neutron fraction. To assure the reactor controllability and safety, the delayed neutron fraction should be sufficiently large. Table 7 shows the average delayed neutron fractions, the ν -value (i.e., number of produced neutrons per fission), the fission rates and the weighted delayed neutron fraction for actinide nuclides. These values were calculated by using the BETA-K code developed at KAERI (Kim et al., 1998). The weighted fractional delayed neutron fraction for each nuclide in this table is given by

$$\beta_{f,i} = \frac{\nu_i \beta_i F_i}{\sum_j \nu_j F_j}$$

where F_i means the fission rate of the i th nuclide.

In Table 7, the total delayed neutron fraction (β_{total}) is the summation of the weighted fractional delayed neutron fractions. On the other hand, the effective delayed neutron fraction (β_{eff}) is calculated by taking into account the adjoint flux and the energy spectra of delayed neutrons and prompt neutrons. The effective delayed neutron fraction (β_{eff}) is given by

$$\beta_{\text{eff}} = \frac{\sum_m \sum_{i=1}^6 \beta_{im} \int \sum_g \phi_g^* \lambda_{dg} \sum_{g'} (\nu \Sigma_f)_{mg'} \phi_{g'} dV}{\int \sum_g \phi_g^* \lambda_g \sum_{g'} (\nu \Sigma_f)_{g'} \phi_{g'} dV}$$

Table 7
Analysis of the contributions of actinides to the delayed neutron fraction

Nuclides	β_i	ν_i	CORE-I (PWR TRU)		CORE-II (DB-MHR TRU)	
			Fission rate ($\times 10^{20}$)	Weighted $\beta_{f,i}$ ($\times 10^{-4}$)	Fission rate ($\times 10^{20}$)	Weighted $\beta_{f,i}$ ($\times 10^{-4}$)
²³⁴ U	0.00506	2.549	0.173	0.1166	0.578	0.4443
²³⁵ U	0.00676	2.472	0.221	0.1930	0.602	0.5992
²³⁶ U	0.00891	2.604	0.015	0.0186	0.051	0.0707
²³⁸ U	0.01598	2.753	3.991	9.1625	4.089	10.7144
²³⁸ Pu	0.00138	3.020	3.493	0.7619	7.364	1.8331
²³⁹ Pu	0.00218	2.965	33.742	11.3569	17.617	6.7670
²⁴⁰ Pu	0.00298	3.024	9.848	4.6249	7.075	3.7920
²⁴¹ Pu	0.00544	2.978	8.335	7.0457	6.685	6.4493
²⁴² Pu	0.00643	3.066	1.898	1.9515	7.325	8.5930
²³⁷ Np	0.00376	2.873	0.766	0.4319	0.859	0.5530
²⁴¹ Am	0.00122	3.491	0.841	0.1874	0.913	0.2322
^{242m} Am	0.00208	3.324	0.594	0.2139	0.616	0.2533
²⁴³ Am	0.00224	3.548	0.462	0.1917	2.153	1.0192
β_{total}			0.00363		0.00413	
β_{eff}			0.00304		0.00310	

In the above equation, ϕ_g and ϕ_g^* represent the g th group forward and adjoint neutron fluxes, respectively.

As shown in Table 7, β_{eff} is significantly smaller than β_{total} , because the spectrum of the delayed neutrons is significantly softer than the core average spectrum and the neutron importance (i.e., adjoint flux) increases with the neutron energy. ²³⁸U has the largest β value and both ²⁴¹Pu and ²⁴²Pu have a substantially larger β value than ²³⁹Pu. In the LWR TRU core, ²³⁹Pu is the largest contributor to the delayed neutron fraction, while it is only a minor contributor in the DB-MHR TRU core. ²⁴²Pu is the 2nd biggest contributor to the β value in the DB-MHR TRU core, while its fission rate is quite small in the LWR TRU core. Consequently, the β_{total} value is significantly larger in the DB-MHR TRU core than in the LWR TRU core. However, the β_{eff} of the DB-MHR TRU core is only marginally larger than that of the LWR TRU core due to the harder neutron spectrum. On the other hand, the DB-MHR TRU core has a shorter neutron life time by $\sim 19\%$ and it leads to a $\sim 25\%$ larger inverse period, which means a faster transient for the same reactivity insertion in the DB-MHR TRU core. The shorter neutron life time of the DB-MHR TRU core is mainly due to the higher capture probability of neutrons in the core.

4. Modifications for improved core safety

In the previous section, it was found that the SFR core fed by the DB-MHR has a substantially higher sodium void worth as well as a lower control rod worth. In this section, several design variants to the DB-MHR SFR core (CORE-II) are considered to increase the control rod worth and to reduce the sodium void worth.

To increase the control rod worth, we evaluated two design modifications: (1) lower boron enrichment

Table 8
Comparison of the core performances of the alternative designs for improving the control rod worth

Parameters	Reference	Design-A1	Design-A2
¹⁰ B wt% in the central B ₄ C shields	90.0	19.5	N/A (sodium ducts)
Burnup reactivity swing (pcm)	2851	2847	2754
Conversion ratio (fissile)	0.8651	0.8698	0.8830
Average discharge burnup (MWD/kg)	119.0	119.0	119.0
TRU wt% in HM (BOEC)	50.9	50.2	47.8
TRU consumption rate (kg/GWtEFPY)	251.9	247.0	234.0
Average power density (W/cc)	302.1	302.1	302.1
3D power peaking factor (BOEC/EOEC)	1.47/1.44	1.47/1.43	1.44/1.40
Peak fast neutron fluence (n/cm ²)	3.45×10^{23}	3.45×10^{23}	3.47×10^{23}
Sodium void worth (BOEC, pcm)	1777	1795	1838
Control rod worth (BOEC, pcm)	6330	6569	7488

(19.5 wt% – natural boron) in the central B₄C shield assemblies, and (2) removal of the central B₄C shield assemblies. In the latter case, the shield assemblies are replaced by sodium ducts. Table 8 shows the effects of the design modifications on the core performance parameters and the radial power distribution without the central shield assemblies is shown in Fig. 5. From Table 8, it is observed that the natural B₄C shield assemblies slightly improves the control rod worth while a complete removal of the shield block significantly increases the rod worth, by ~1100 pcm. Removal of the central shield block also results in a slightly higher sodium void worth and a reduced power peaking factor. The reduced power peaking without the central shield blocks indicates that the shield assemblies do not help flatten the radial power distribution.

Three design modifications were considered to reduce the sodium void worth: (1) reduction of the active core height, (2) increase of the fuel rod diameter, and (3) increase of the number of ZrH_{1.8} moderator rods. Table 9 shows the results of the investigation. The Design-B1 core has a reduced core height of 70 cm, and uses a larger fuel rod of 8.0 mm diameter (original diameter = 7.5 mm).

The Design-B2 core has the same height as that of the Design-B1 core, but it uses a larger fuel diameter of 8.5 mm. In the Design-B3 core, the core height is reduced further to 60.0 cm, keeping the fuel diameter at 8.5 mm. The last core (Design-B4) is identical to Design-B3 except that 12 moderator rods are used in each fuel assembly to soften the neutron spectrum. For all the cores in Table 9, the wire wrap diameter was reduced from 1.6 mm to 1.4 mm in order to reduce the lattice pitch-to-diameter ratio.

Table 9 shows that the sodium void worth can be effectively reduced by reducing the core height and (or) by increasing the fuel rod diameter. It is also noted that softening the neutron spectrum clearly provides a reduced sodium void worth. The control rod worth is also reduced in the four design modifications due to the reduced core height. Based on the results in Table 8, the control rod worth can be substantially increased by replacing the central B₄C shield zone with the sodium ducts. In Table 9, Design-B4 provides the least sodium void worth of 1064 pcm (~3.4\$), which is smaller by ~700 pcm than that of the reference core (CORE-II). However, it is still larger

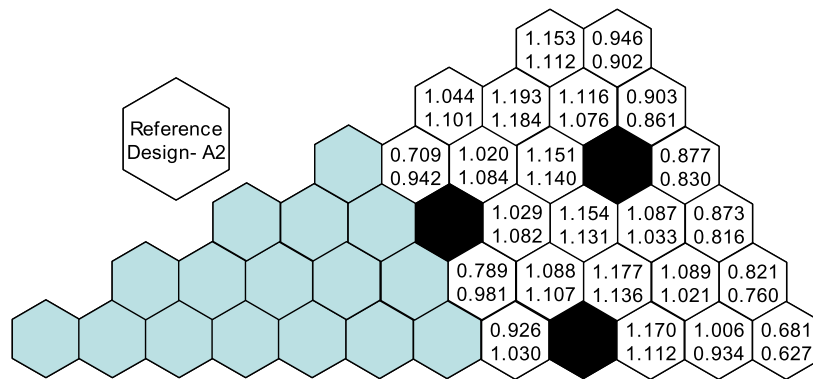


Fig. 5. Impact of the central B₄C shield on the radial power distribution (reference with B₄C shield, Design-A2 without B₄C shield).

Table 9
Comparison of the core performances of the alternative designs for improving the sodium void worth

Parameters	Design-B1	Design-B2	Design-B3	Design-B4
Core height (cm)	70.0	70.0	60.0	60.0
Fuel rod diameter (mm)	8.0	8.5	8.5	8.5
Number of ZrH _{1.8} rods/FA	6	6	6	12
Lattice P/D ratio	1.188	1.176	1.176	1.176
Burnup reactivity swing (pcm)	2819	2350	2879	2862
Conversion ratio (fissile)	0.8755	0.8997	0.8704	0.8723
Average discharge burnup (MWD/kg)	117.6	102.2	119.3	122.0
TRU wt% in HM (BOEC)	47.8	42.5	48.4	50.3
TRU consumption rate (kg/GWtEFPY)	240.9	214.0	244.5	249.0
Average power density (W/cc)	326.0	296.6	345	346
3D power peaking factor (BOEC/EOEC)	1.47/1.43	1.48/1.45	1.47/1.43	1.47/1.43
Peak fast neutron fluence (n/cm ²)	3.54 × 10 ²³	3.27 × 10 ²³	3.58 × 10 ²³	3.27 × 10 ²³
Sodium void worth (BOEC, pcm)	1435	1363	1216	1064
Control rod worth (BOEC, pcm)	5785	5819	5149	4946
Effective delayed neutron fraction	0.00315	0.00322	0.00314	0.00313
Doppler coefficient (pcm/K, at 900 K)	-0.234	-0.276	-0.221	-0.344
Sodium density coefficient (pcm/K)	0.413	0.384	0.325	0.285
Neutron life time (micro sec)	0.280	0.286	0.276	0.300

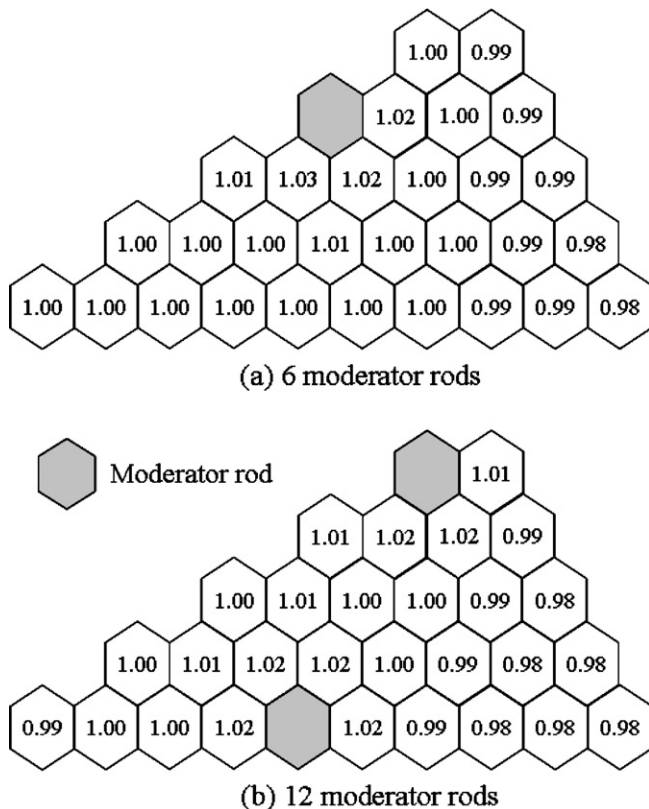


Fig. 6. Impact of the moderator rods on assembly power distribution.

than that of the LWR TRU case ($\sim 1.3\%$). In Table 9, it is worthwhile to note that Design-B4 provides a much smaller sodium density coefficient and a much more negative Doppler feedback than in the reference CORE-II design. Also, Table 9 shows that the spectrum softening by using the moderator rods leads to a slightly longer neutron life time.

The impact of the $ZrH_{1.8}$ moderator rods on the assembly power distribution has been evaluated by the MCNP code (Briesmeister, 1999) and the results are provided in Fig. 6. In the evaluation, the fuel composition was taken from the BOEC condition of the equilibrium cycle of Core-II in Table 6. It is clearly observed that the local power peaking is quite small, 1.03 for six moderator rods and 1.02 for 12 moderator rods.

In spite of the improved sodium void worth, the modified cores have a higher linear heat generation rate than the reference case since the core height is reduced and (or) the number of fuel rods is reduced. For implementation of the design measure (or measures), detailed thermal-hydraulic analyses of the core should be performed to ensure integrity of the fuel.

5. Summary and conclusions

A synergistic combination of a DB-MHR and a metal-fueled SFR has been considered for an efficient transmutation of TRUs from LWRs. In this concept, the LWR TRUs are deeply transmuted (discharge burnup $\sim 63.5\%$)

in a DB-MHR core and the spent fuel of DB-MHR is reprocessed and recycled into an SFR transmuter with a closed fuel cycle. A synergy SFR core has been designed and its characteristics have been compared with those of a conventional SFR core directly loaded with LWR TRUs. For a consistent comparison, the two SFR cores have been designed to have the same TRU consumption rate.

It has been confirmed that the MHR–SFR synergy fuel cycle is possible from the neutronics point of view, in spite of an extremely high fuel burnup in the DB-MHR core: actinides of the DB-MHR spent fuel can be used as a feed material in the synergy SFR core. We have found that a synergy SFR has a smaller burnup reactivity swing, a higher delayed neutron fraction, but also a more positive sodium void worth and a less negative Doppler coefficients and a smaller control rod worth than the one fed with LWR TRUs. The net control rod worth is greater in the DB-MHR TRU core due to the smaller reactivity swing. The fuel and core expansion coefficients were found to be strictly negative and comparable for the two SFR cores. Taking into account the sodium density, the Doppler, the fuel expansion, the radial core expansion coefficients, the net temperature feedback effect is negative in both LWR and DB-MHR TRU cases, and the LWR TRU case has a more negative net temperature coefficient. It was also found that the sodium void worth of the DB-MHR TRU core can be effectively reduced by adopting combinations of reduced core height, thicker fuel rods, or more moderator rods.

In this work, only the neutronic characteristics of the synergy SFR core have been evaluated. In order to fully address the feasibility of the MHR–SFR synergy fuel cycle, additional work on the fuel and safety characteristics of the core will be necessary including the determination of an optimal TRU burnup in the DB-MHR core that feeds the subsequent synergy SFR core.

References

- Baxter, A., Rodriguez, C., Venneri, F., 2001. The application of gas-cooled reactor technologies to the transmutation of nuclear waste. *Progress in Nuclear Energy* 38, 81.
- Briesmeister, J.F. (Ed.), 1999. MCNP4C-A General Monte Carlo N-Particle Transport Code System. CCC-660, Los Alamos National Laboratory.
- Del Cul et al., 2002. TRISO-Coated Fuel Processing to Support High-Temperature Gas-Cooled Reactors. ORNL/TM-2002/156, Oak Ridge National Laboratory.
- Derstine, K.D., 1984. DIF3D: A Code to Solve One-, Two-, and Three-Dimensional Finite Difference Diffusion Theory Problems, ANL-82-64, Argonne National Laboratory.
- Hill, R.N., Wade, D.C., Riaw, J.R., Fujita, E.K., 1995. Physics studies of weapons plutonium disposition in the integral fast reactor closed fuel cycle. *Nuclear Science and Engineering* 121, 17.
- Hofman, G.L., Walters, L.C., Bauer, T.H., 1997. Metallic fast reactor fuels. *Progress in Nuclear Energy* 31, 83.
- Hong, S.G., Kim, S.J., Kim, Y.I., 2008. Annular type fast reactor cores with low sodium void worth for TRU burning. *Nuclear Technology* 162, in press.
- Kim, T.K. et al., 1998. Development of an Effective Delayed Neutron Fraction Calculation Code, BETA-K, KAERI/TR-1120/98.

- Kim, J.D., 2001. KAFAX-E66, Calculation Note NDL-23/01, Nuclear Data Evaluation Laboratory Internal Report, Korea Atomic Energy Research Institute.
- Kim, Y., Venneri, F., 2007. Optimization of TRU Burnup in Modular Helium Reactor, ICAPP'07, Nice, France, May 13–18.
- Leggett, R.D., Walters, L.C., 1993. Status of LMR fuel development in the United States of America. *Journal of Nuclear Material* 204, 23.
- MacFarlane, R.E., 1993. TRANSX 2: A Code for Interfacing MATXS Cross Section Libraries to Nuclear Transport Codes. LA-12312-MS, Los Alamos National Laboratory.
- Messaoudi, N., Tommasi, J., 2002. Fast burner reactor devoted to minor actinide incineration. *Nuclear Technology* 137, 84.
- Newton, T.D., Smith, P.J., 2003. A moderated target sub-assembly design for minor actinide transmutation. In: *Proceedings of GLOBAL2003*, New Orleans, LA, USA, November 16–20.
- Toppel, B.J., 1983. A User's Guide to the REBUS-3 Fuel Cycle Analysis Capability. ANL-83-2, Argonne National Laboratory.
- Vavilov, S., Kobayashi, T., Myochin, M., 2004. Principle and test experience of the RIAR's oxide pyroprocess. *Journal of Nuclear Science and Technology* 41 (10), 1018.
- Wakabayashi, T., Takahashi, K., Yanagisawa, T., 1997. Feasibility studies on plutonium and minor actinide burning in fast reactors. *Nuclear Technology* 118, 14.